UNIVERSITÀ DEGLI STUDI DI BARI

Dipartimento Interateneo di Fisica M. Merlin

PhD School in Physics XXXII Cycle

II year activity report

CMS-RPC system upgrade project for the phase II of LHC

Supervisor: Dr.ssa G. Pugliese

PhD student: A. Gelmi

My PhD research activity is developing in the context of the muon upgrade project of the Compact Muon Solenoid (CMS) experiment for the High Luminosity phase of the Large Hadron Collider (HL-LHC) at CERN. In particular my activity is focusing on the upgrade of the Resistive Plate Chambers (RPC) system.

1 CMS-RPC system upgrade

At present, three types of gas-ionization detectors make up the CMS muon system [1]: Drift Tube chambers (DT), Cathode Strip Chambers (CSC), and Resistive Plate chambers (RPC). The RPC system [2] covers both Barrel and Endcap regions of CMS contributing to the trigger, reconstruction and identification of muons. It consists of 1056 RPCs, organized in 4 stations called RB1 to RB4 in the Barrel region, and RE1 to RE4 in the Endcap region.

The RPC system was designed to provide muon identification, excellent triggering, timing and momentum measurements at the Large Hadron Collider (LHC) at the nominal luminosity of 1×10^{34} cm^{-2}s^{-1}. During the LHC Run1 and Run2 data taking the performance of the muon systems was outstanding [3].

In the second phase of the LHC physics program, HL-LHC, the instantaneous luminosity will reach 5×10^{34} cm^{-2}s^{-1} (factor five more then the nominal LHC luminosity), providing to CMS an additional integrated luminosity of about 3000 fb^{-1} over 10 years of operation, starting in 2026. The expected conditions in terms of background, pile-up and the probable aging of the present detectors, will make the muon identification and correct p_T assignment a challenge for the muon system. In order to ensure redundancy of the muon system [3] also under the HL-LHC conditions, two upgrades [4] are planned on the RPC system: the consolidation of the present system and the extension of the muon coverage at the $|\eta| < 2.4$.

1.1 Longevity study for the present RPC system

The present RPC system has been certified for 10 LHC years operation, at a maximum background rate of 300 Hz/cm^2 and a total integrated charge of 50 mC/cm^2 [1].

Based on Run2 data and assuming a linear dependence of the background rates as a function of the instantaneous luminosity, the expected background rates and integrated charge at HL-LHC will be respectively $\approx$ 600 Hz/cm^2 and $\approx$ 840 mC/cm^2, (including a safety factor of three) [4]. HL-LHC will therefore be a challenge for the RPC system since the new operating conditions are much higher with respect to those for which the detectors had been designed, and could induce non-recoverable aging effects that can alter the detector properties and performance.
A new longevity test is then needed to estimate the impact of the HL-LHC conditions up to an integrated charge equivalent to the integrated luminosity of 3000 fb^{-1}, in order to confirm that the RPC system will survive to the expected HL-LHC conditions. Longevity studies will identify possible aging effects by monitoring the main detector parameters and performance as a function of the integrated charge.

A dedicated longevity study was set up at the CERN Gamma Irradiation Facility (GIF++) [5] where it is possible to test full size detectors. The facility is equipped with a 13 TBq Cs-137 gamma source and a system of movable filters allows to varying the gamma flux, providing a fairly realistic simulation of the HL-LHC background conditions. A 100 GeV muon beam, providing an excellent probes for detector performance studies, complements the source.

In July 2016, four spare Endcap chambers (two RE2/2 and two RE4/2 chambers) have been installed at GIF++. Two chambers out of the fours (one RE2/2 and one RE4/2), are continuously operated under gamma irradiation, while the remaining two chambers are turned on only from time to time and used as reference.

At present, about 431 mC/cm^2 and 218 mC/cm^2 have been integrated for RE2/2 and RE4/2 irradiated detectors, which corresponds respectively to approximately 51% and 26% of the expected HL-LHC integrated charge.

Since the beginning of the irradiation test, I am in charge to monitor the detector parameters (counting rates and currents at different background conditions, noise and dark current, electrode resistivity, etc.).

1.1.1 Detector parameters monitoring

In order to spot possible degradations of the electrodes surface due to the irradiation, the detector noise rate and dark current are periodically measured. Figure 1 shows the currents (left) and noise rate (right) at the working point as a functions of the integrated charge for the RE2/2 irradiated and reference chambers. No significant variations have been observed so far.

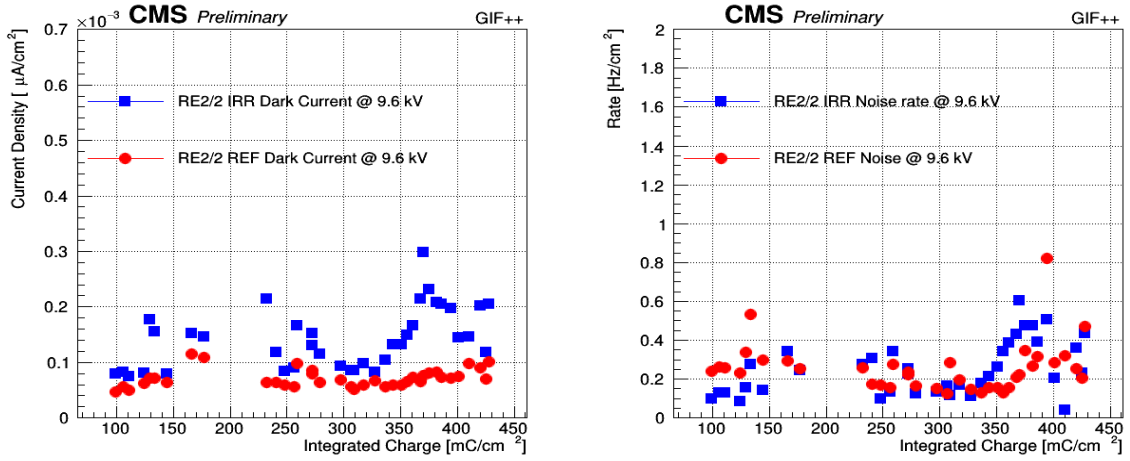

Figure 1: Dark current (lef) and noise rate (right) versus the integrated charge, for RE2/2 irradiated (blues) and reference (red) chamber, at the working point voltage.

The current and rate with background radiation are periodically measured as well. To exclude the dependence on the external parameters, the ratios of the irradiated and the reference chambers is measured as a function of the integrated charge. Figure 2 left shows the RE2/2 current and rate ratio.

The measurements show a decreasing trend at the beginning of the irradiation period, up to $\approx 300 mC/cm^2$, when the operating conditions, in terms of gas flow rate and relative gas humidity were too low with respect to the high gamma background rate. These operating conditions leads to the electrodes' resistivity increase, which caused the observed rate and current decrease.

The electrodes' resistivity increase is confirmed by the measurements performed running the RPCs filled with pure Argon gas. Figure 2 right shows the coherent correlation between the RE2/2 currents ratio (red) and the resistivity variation (blue). The resistivity variation allow us to cancel out the dependence on the environmental conditions, and is defined as:

$$\rho_{var} = \frac{\rho_{irr} - \rho_{ref}}{\rho_{irr}} \tag{1}$$

These plots show also that the resistivity increase is a recoverable effect, in fact the resistivity start to decrease, and the current and rate to increase, when the gas flow and the gas relative humidity have been increased.

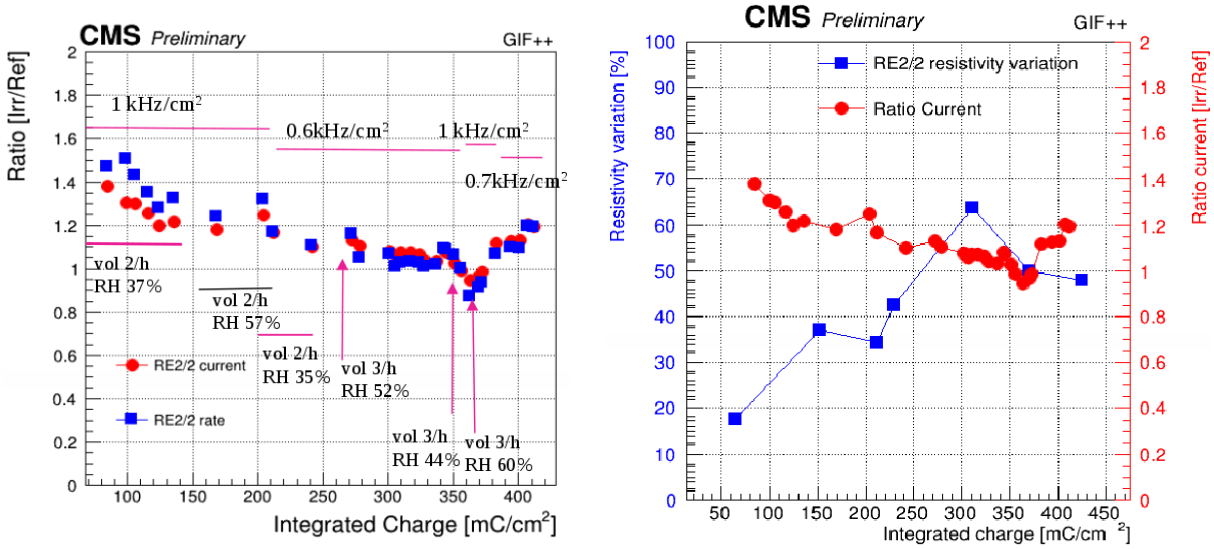

Figure 2: Left: RE2/2 current (red) and rate (blues) ratio between irradiated and reference chamber as a function of the integrated charge. Right: RE2/2 current ratio (red) and resistivity variation (blue).

1.1.2 Detector performance monitoring

The detector performance has been tested using the muon beam, before starting the longevity test and repeated after different irradiation periods at GIF++, up to 51% of the expected integrated charge. Figure 3 shows the RE2/2 irradiated chamber efficiency as a function of the effective High Voltage (voltage normalized at the standard temperature and pressure), without irradiation (left), and with a gamma background rate of $\approx 600 Hz/cm^2$ (right).

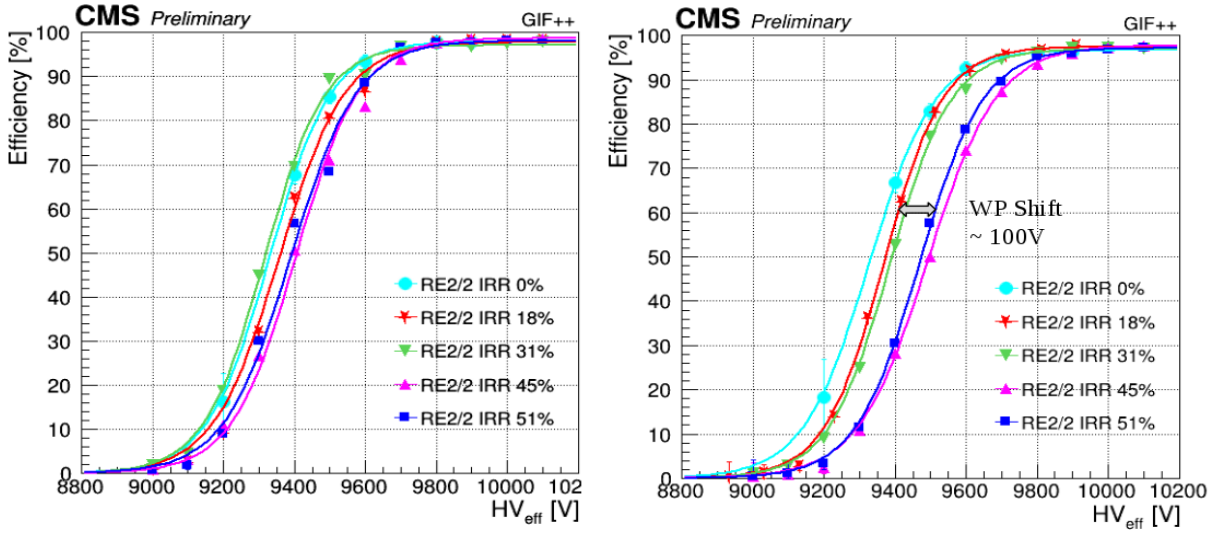

Figure 3: RE2/2 irradiated chamber efficiency as a function of the effective HV, taken with no irradiation (left) and under a gamma background rate of about $600 Hz/cm^2$ (right). The efficiency is measured during different Test Beams (TB) corresponding to different fractions of the target charge to integrate.

The performance without background rate is stable in time and we do not observe any

efficiency degradation or working point shift. With a background rate of $\approx 600 Hz/cm^2$ the efficiency remains stable at working point, but we observe an 100 V shift, starting from 45% of the expected integrated charge.

The working point shift is related to the electrodes' resistivity increase, since the effective voltage applied to the electrodes (HV) is reduced by the voltage drop across the electrodes, which is proportional to the current (I) produced by the ionizing particles and to the bakelite resistance (R) [6]. The effective voltage applied to the gas (HV_{gas}) is therefore defined as:

$$HV_{gas} = HV - RI \tag{2}$$

The detector operation regime is invariant with respect to HV_{gas}, therefore the efficiency as a function of HV_{gas} does not depends anymore on the background radiation and on the bakelite resistance. Figure 4 left represent the RE2/2 irradiated chamber efficiency curves at different background radiation (up to $\approx 600 Hz/cm^2$) and at different integrated charge. All the efficiency curves overlap and we do not observe anymore the working point shift, since the electrodes' resistivity increase effect has been removed.

The RE2/2 irradiated chamber efficiency at the working point as a function of the background rate is shown in Fig. 4 right. The efficiency is stable in time with a 2% decrease at the highest expected background rate, 600 Hz/cm^2.

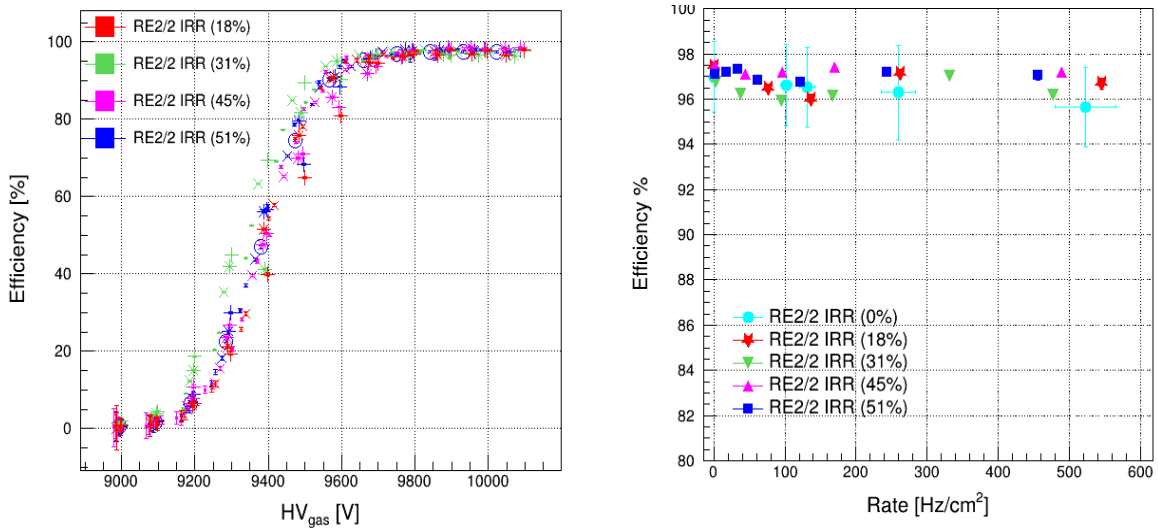

Figure 4: Left: RE2/2 irradiated chamber efficiency as a function of the HV gas, at different background irradiations and at different integrated charge values. Right: RE2/2 irradiated chamber efficiency at working point as a function of the background rate at different integrated charge values.

From preliminary results no evidence of any aging effect has been observed so far. The main detectors parameters are stable, unless minor variations like the electrodes' resistivity, that did not affected the performance which remains stable up to 51% of the expected integrated charge. Further investigations are needed to get closer to the final integrated charge of 840 mC/cm^2.

1.2 RPC system extension at the high eta region $1.8 < |\eta| < 2.4$

In view of the HL-LHC the RPC system will extend the muon eta acceptance from $|\eta| = 1.9$ to 2.4 in order to complement the existing ME3-4/1 stations, equipped with CSC only, increasing the muon system redundancy, and to extend the contribution of RPCs for both muon tracking and triggering in the forward region.

The two Endcap stations RE3-4/1 will be equipped with a new generation of improved RPC (iRPC) [7]. The extensive R&D activity allowed to define the baseline for the new iRPC detectors, which are based on the RPC technology, but having lower electrodes resistivity, $0.9 \div 3 \times 10^{10} \Omega cm$, and thinner electrodes and gas gap thickness, equal to 1.4 mm with respect to the 2 mm of the current RPCs, with the aims to improve the rate capability in order to cope the harsher expected background rate conditions.

1.2.1 iRPC background rate study

During the II Phd year, I performed a study to accurately estimate the expected background hit rate R(E) during the future HL-LHC runs in the forward region RE3-4/1, where will be installed the new iRPC. The estimation of the background hit rate is done scaling the incident background fluxes ϕ_{bkg} with the iRPC sensitivity S(E).

$$R(E) = \phi_{bkg} \times S(E) \tag{3}$$

The sensitivity represent the detectors response to the background particles, and is defined as the probability for a particle N_{bkg} at a givewhichn energy reaching the detector surface, to produce a signal N_{HIT}:

$$S(E) = \frac{N_{HIT}}{N_{bkg}}(E) \tag{4}$$

The sensitivity is a function of the energy of the incoming particles, because at different energies, different processes are responsible for the production of secondary particles. The GEANT [8] Monte Carlo simulation allowed me to study the sensitivity of the iRPCs at HL-LHC background conditions, considering the different particles (gammas, neutrons and electrons) and energy spectrum.

The detector sensitivity depends also from the detector geometry. The detector geometry which I described in the GEANT simulation code corresponds to the first large size iRPC prototype [7] that has been tested at GIF++. The double gap geometry, having 1.4 mm thickness of gas volume and electrodes, was employed with the strip plane sandwiched between the two gas gaps. In order to properly include the secondary radiations produced by high energy particles, all the outer layers of materials composing the trapezoidally shaped detector body (height = 1613 mm , long side = 866.3 mm, short side = 584.1 mm) are also implemented in the simulation code.

I already performed last year the detector geometry validation, when I studied the sensitivity of the same iRPC prototype at the GIF++ gamma energy, both by Monte Carlo simulated method and experimentally. Figure 5 shows the detector sensitivities to ^{137}Cs gammas measured at GIF++ at different background conditions (ABS) compared with the simulated sensitivity. A 100 keV energy thresholds on the primary and secondary charged particles that produce a signal in the gas gap allows to obtain a good agreement between experimental and simulated data and to validate the detector geometry.

For the sensitivity study I used GEANT 4.9.6 version, with the "FTFP-BERT-HP" package to describe the physics processes, since it includes all the standard electromagnetic processes and

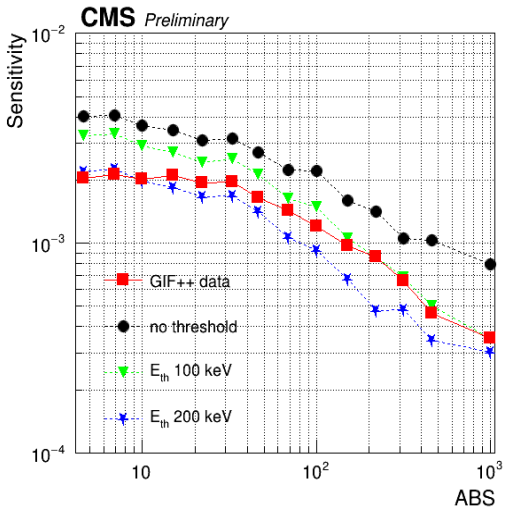

Figure 5: Detector sensitivities to ^{137}Cs gammas measured at GIF++ at different background conditions (ABS) compared with the simulated sensitivity: without energy threshold, with energy thresholds of 100 keV and 200 keV.

it is the most accurate neutron model, especially at low energies. For the GEANT simulation some assumptions [9] have been applied:

- The particle source is isotropic and particles randomly strike the detector.
- An energy threshold of 100 keV has been applied to the primary and secondary charged particles that produce a signals in the gas gaps. The realistic threshold value of 100 keV was empirically obtained from the iRPC geometry validation study comparing the measured gamma rate at GIF++ and the simulated rate (Fig. 5).
- If more than one charged particles reach the gas gap, only the first one is assumed to generate a signal.

In order to obtain a statistical uncertainty less than 1%, I simulated a large numbers of events (3×10^6 for each energy value). The estimation of the sensitivity variance is given by a binomial distribution.

Fig.6 shows the results of the iRPC sensitivity with respect to the different background particles (neutrons, gammas, electrons and positrons), at the expected HL-LHC spectra.

The neutron sensitivity values rise in the low energy region ($E_n < 10^{-5}$ MeV), which is mostly due to gammas coming from the (n,γ) capture reaction whose cross section increases with decreasing in neutron energy as $\sigma \propto 1/\sqrt{E_n}$.

For the neutron sensitivity we observe the main impact of the applied 100 keV energy threshold ($\approx$ 17% less), as shown in Fig. 6, especially at the energy region $10^{-4} < E < 1\ MeV$. For the gammas particles the difference is $\approx$ 4%, and for electrons and positrons $\approx$ 6%. In total the applied threshold decrease the detector sensitivity of $\approx$ 10%.

Finally I estimated the expected background hit rate in the RE3-4/1 stations during HL-LHC scaling the incident particles flux with the iRPC sensitivity. The incident fluxes for the different background particles are estimated implementing the upgraded CMS geometry and the accelerator conditions for proton-proton collisions in the FLUKA simulation code (CMS Fluka study version v.3.7.7.0). In the present background simulations, we assume a centre of mass energy of 14 TeV with a nominal instantaneous luminosity of $5{\times}10^{34}\mathrm{cm}^{-2}\mathrm{s}^{-1}$.

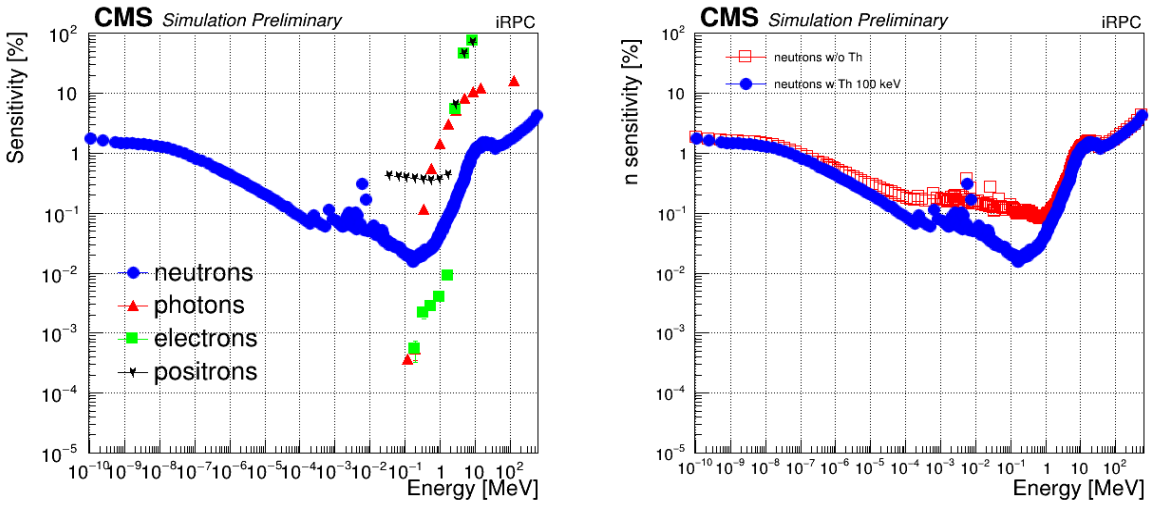

Figure 6: Left: iRPC sensitivity with respect to the different background particles (neutrons, photons, electrons and positrons) as a function of the incident particles energy. Right: iRPC neutron sensitivity sensitivity without any energy threshold for the charged particles that produce a signals in the gas gaps (red), and with an energy threshold of 100 keV (blue).

Figure 7 left shows the expected background hit rate as a function of the incident particles energy, estimated from the convolution of the sensitivities and the incident particles fluxes.

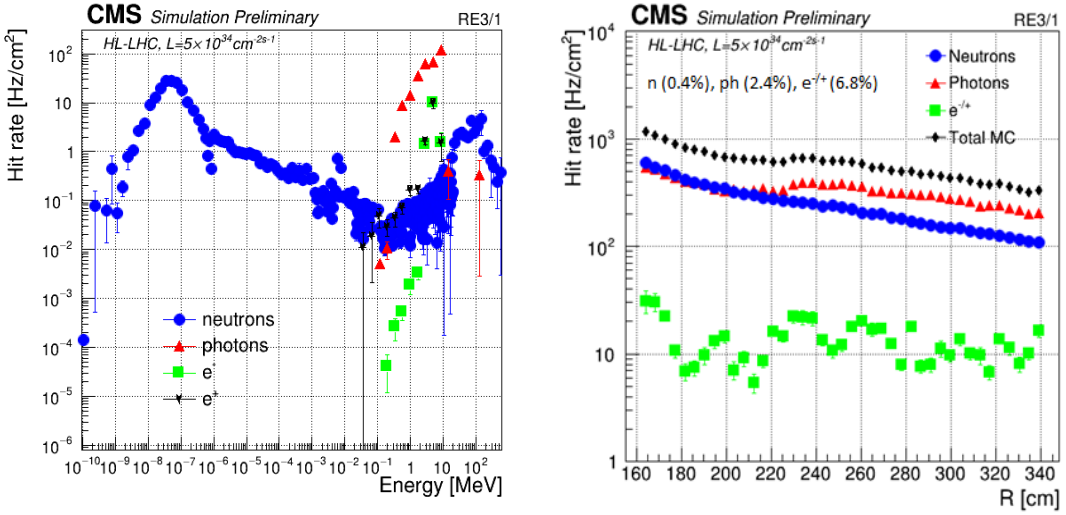

Figure 7: Left: Background hit rate expected in the RE3/1 station during HL-LHC as a function of the energy of the incoming particles. Right: Expected background hit rate in the RE3/1 station during HL-LHC as a function of R.

I used then the average sensitivity values, [n (0.4%), γ (2.4%), $e^{-/+}$ (6.8%)], to estimate the background hit rate as a function of the distance from the centre of the CMS beam pipe. Figure 7 right shows the contribution of the different particles to the total background hit rate in the RE3/1 station as a function of the distance from the centre of the CMS beam pipe. The average background rate of $\approx$ 600 Hz/cm^2 indicates the requirement of a minimum rate capability of $\approx$ 2 kHz/cm^2 for the iRPCs when considering a safety factor of three.

References

[1] CMS Collaboration, *The CMS muon project: Technical Design Report*, CERN, Geneva Switzerland, LHC Experiments Committee (1997) [CMS-TDR-3]

[2] G. Pugliese [CMS Muon Collaboration], *The RPC system for the CMS experiment*, 2006 IEEE NSS Conference Record N24-3, January 2007.

[3] A. M. Sirunyan *et al.* [CMS Collaboration], *Performance of the CMS muon detector and muon reconstruction with proton-proton collisions at* $\sqrt{s} = 13$ *TeV*, [arXiv:1804.04528 [physics.ins-det]].

[4] CMS Collaboration, *The Phase-2 Upgrade of the CMS Muon Detectors*, CERN, Geneva Switzerland, LHC Experiments Committee (2017) [CMS-TDR-016]

[5] R. Guida [EN and EP and AIDA GIF++ Collaborations], *GIF++: A new CERN Irradiation Facility to test large-area detectors for the HL-LHC program*, PoS ICHEP **2016** (2016) 260.

[6] G. Pugliese *et al.*, *Aging study for resistive plate chambers of the CMS muon trigger detector*, Nuclear Instruments and Methods in Physics Research A 515 (2003) 342347.

[7] K.S. Lee *et al.*, *Thin Double-gap RPCs for the Phase-2 Upgrade of the CMS Muon System, CERN, Geneva Switzerland* [CMS-NOTE-2017-005]

[8] S. Agostinelli *et al.* [GEANT4 Collaboration], *GEANT4: A Simulation toolkit*, Nucl. Instrum. Meth. A **506** (2003) 250. doi:10.1016/S0168-9002(03)01368-8

[9] J. T. Rhee *et al.*, *Study of the neutron sensitivity for the double gap RPC of the CMS/LHC by using GEANT4*, J. Korean Phys. Soc. **48** (2006) 33.

2 Schools and Conferences

2.1 Schools

- RD51 Gaseous detectors lectures, 11-15 December 2017, CERN, Switzerland
- First International RPC detector school, 14-17 February 2018, Mexico City, Mexico
- XXX National seminar of nuclear and subnuclear physics, 5-12 June 2018, Otranto, Italy
- CMS Machine Learning workshop, 2-4 July 2018, CERN, Switzerland

2.2 International conferences

- XIV Workshop on Resistive Plate Chambers and Related Detectors (RPC 2018), 19-23 February 2018, Puerto Vallarta, Mexico
  Oral presentation: *"Longevity studies for the CMS-RPC system"*
- Incontri di Fisica dele Alte Energie IFAE 2018, 4-6 April 2018, Milano, Italy
  Oral presentation: *"RPC upgrade project for CMS Phase II"*
- 14th Pisa Meeting on Advanced Detectors PM2018, 27 May - 2 June 2018, La Biodola, Isola d'Elba, Italy
  National conference. Poster: *"Background rate study for the CMS improved-RPC at HL-LHC using GEANT4"*

3 Publications

3.1 First author publications

- **"Longevity studies for the CMS-RPC system"**
  A. Gelmi et al., JINST, JINST-017P-0818, Proceeding of: "XIV Workshop on Resistive Plate Chambers and Related Detectors". Under review.
- **"Background rate study for the CMS improved-RPC at HL-LHC using GEANT4"**
  A. Gelmi et al. (on behalf of the CMS collaboration), Nucl. Instrum. Meth., NIMA-D-18-00307R1, Proceeding of: "14th Pisa Meeting on Advanced Detectors PM2018". Already reviewed, going to print.

3.2 RPC publications

- "RPC upgrade project for CMS Phase II",
  M.I. Pedraza et al., CMS Collaboration, JINST, Proceeding of: XIV Workshop on Resistive Plate Chambers and Related Detectors.
- "R&D results of iRPC tested at GIF++ for CMS Phase II upgrade",
  J. H. Lim et al., CMS Collaboration, JINST, Proceeding of: XIV Workshop on Resistive Plate Chambers and Related Detectors.
- "Fast timing measurement for CMS RPC Phase II upgrade",
  C. Combaret et al., CMS Collaboration, JINST, Proceeding of: XIV Workshop on Resistive Plate Chambers and Related Detectors.

- "RPC Radiation Background Simulations for the High Luminosity Phase in the CMS Experiment",
  B. Carpinteyro et al., CMS Collaboration, JINST, Proceeding of: XIV Workshop on Resistive Plate Chambers and Related Detectors.

- "CMS RPC background studies during LHC run II",
  R. Trejo et al., CMS Collaboration, JINST, Proceeding of: XIV Workshop on Resistive Plate Chambers and Related Detectors.

- "High rate, high time precision RPC detector for LHC",
  F. Lagarde et al., CMS Collaboration, JINST, Proceeding of: XIV Workshop on Resistive Plate Chambers and Related Detectors.

- "The CMS RPC Detector Status and Operation at LHC",
  M.Shah et al., CMS Collaboration, JINST, Proceeding of: XIV Workshop on Resistive Plate Chambers and Related Detectors.

- "Test of a real-size Mosaic MRPC developed for CMS muon upgrade",
  Y. Yu et al., CMS Collaboration, JINST, Proceeding of: XIV Workshop on Resistive Plate Chambers and Related Detectors.

- "CMS RPC efficiency measurement using the Tag and Probe method",
  J. Goh et al., CMS Collaboration, JINST, Proceeding of: XIV Workshop on Resistive Plate Chambers and Related Detectors.

- "CMS RPC Integrated Charge",
  M. Cecilia et al., CMS Collaboration, JINST, Proceeding of: XIV Workshop on Resistive Plate Chambers and Related Detectors.

- "The CMS RPC system calibration",
  R. Reyes et al., CMS Collaboration, JINST, Proceeding of: XIV Workshop on Resistive Plate Chambers and Related Detectors.

- "RE3/1 and RE4/1 chambers integration with Forward region of CMS Muon spectrometer",
  E. Voevodina et al., CMS Collaboration, JINST, Proceeding of: XIV Workshop on Resistive Plate Chambers and Related Detectors.

- "CMS RPC Condition Data Automation",
  O. M. Colin et al., CMS Collaboration, JINST, Proceeding of: XIV Workshop on Resistive Plate Chambers and Related Detectors.

- "Search for Heavy Stable Charged Particles in the CMS Experiment using the RPC phase II upgraded detectors",
  G. Sanchez et al., CMS Collaboration, JINST, Proceeding of: XIV Workshop on Resistive Plate Chambers and Related Detectors.

3.3 CMS publications

- CMS Collaboration Author since 11th November 2017 (85 papers)
- **"The Phase-2 Upgrade of the CMS Muon Detectors"**
  CMS Collaboration, CERN-LHCC-2017-012. CMS-TDR-016

All CMS publications list:

References

[1] A. M. Sirunyan *et al.* [CMS Collaboration], "Observation of prompt J/ψ meson elliptic flow in high-multiplicity pPb collisions at $\sqrt{s_{\rm NN}} = 8.16$ TeV," arXiv:1810.01473 [hep-ex].

[2] A. M. Sirunyan *et al.* [CMS Collaboration], "Search for new physics in final states with a single photon and missing transverse momentum in proton–proton collisions at $\sqrt{s} = 13$ TeV," arXiv:1810.00196 [hep-ex].

[3] A. M. Sirunyan *et al.* [CMS Collaboration], "Measurement of exclusive Υ photoproduction from protons in pPb collisions at $\sqrt{s_{\rm NN}} = 5.02$ TeV," arXiv:1809.11080 [hep-ex].

[4] A. M. Sirunyan *et al.* [CMS Collaboration], "Combined measurements of Higgs boson couplings in proton-proton collisions at $\sqrt{s} = 13$ TeV," arXiv:1809.10733 [hep-ex].

[5] A. M. Sirunyan *et al.* [CMS Collaboration], "Search for single production of vector-like quarks decaying to a top quark and a W boson in proton-proton collisions at $\sqrt{s} = 13$ TeV," arXiv:1809.08597 [hep-ex].

[6] A. M. Sirunyan *et al.* [CMS Collaboration], "Jet shapes of isolated photon-tagged jets in PbPb and pp collisions at $\sqrt{s_{\rm NN}} = 5.02$ TeV," arXiv:1809.08602 [hep-ex].

[7] A. M. Sirunyan *et al.* [CMS Collaboration], "Search for invisible decays of a Higgs boson produced through vector boson fusion in proton-proton collisions at $\sqrt{s} = 13$ TeV," [arXiv:1809.05937 [hep-ex]].

[8] A. M. Sirunyan *et al.* [CMS Collaboration], "Search for leptoquarks coupled to third-generation quarks in proton-proton collisions at $\sqrt{s} = 13$ TeV," [arXiv:1809.05558 [hep-ex]].

[9] A. M. Sirunyan *et al.* [CMS Collaboration], "Search for the associated production of the Higgs boson and a vector boson in proton-proton collisions at $\sqrt{s} = 13$ TeV via Higgs boson decays to τ leptons," [arXiv:1809.03590 [hep-ex]].

[10] A. M. Sirunyan *et al.* [CMS Collaboration], "Studies of $\rm B^*_{s2}(5840)^0$ and $\rm B_{s1}(5830)^0$ mesons including the observation of the $\rm B^*_{s2}(5840)^0 \to B^0 K^0_S$ decay in proton-proton collisions at $\sqrt{s}$ =8 TeV," [arXiv:1809.03578 [hep-ex]].

[11] A. M. Sirunyan *et al.* [CMS Collaboration], "Performance of reconstruction and identification of τ leptons decaying to hadrons and ν_τ in pp collisions at $\sqrt{s} = 13$ TeV," JINST **13**, no. 10, P10005 (2018) doi:10.1088/1748-0221/13/10/P10005 [arXiv:1809.02816 [hep-ex]].

[12] A. M. Sirunyan *et al.* [CMS Collaboration], "Search for physics beyond the standard model in high-mass diphoton events from proton-proton collisions at $\sqrt{s} = 13$ TeV," [arXiv:1809.00327 [hep-ex]].

[13] A. M. Sirunyan *et al.* [CMS Collaboration], "Charged-particle nuclear modification factors in XeXe collisions at $\sqrt{s_{\mathrm{NN}}} = 5.44$ TeV," arXiv:1809.00201 [hep-ex].

[14] A. M. Sirunyan *et al.* [CMS Collaboration], "Observation of Higgs boson decay to bottom quarks," Phys. Rev. Lett. **121**, no. 12, 121801 (2018) doi:10.1103/PhysRevLett.121.121801 [arXiv:1808.08242 [hep-ex]].

[15] A. M. Sirunyan *et al.* [CMS Collaboration], "Measurement of jet substructure observables in $\mathrm{t\bar{t}}$ events from proton-proton collisions at $\sqrt{s} = 13$TeV," arXiv:1808.07340 [hep-ex].

[16] A. M. Sirunyan *et al.* [CMS Collaboration], "Search for a charged Higgs boson decaying to charm and bottom quarks in proton-proton collisions at $\sqrt{s} = 8$ TeV," [arXiv:1808.06575 [hep-ex]].

[17] A. M. Sirunyan *et al.* [CMS Collaboration], "Search for pair production of second-generation leptoquarks at $\sqrt{s} = 13$ TeV," [arXiv:1808.05082 [hep-ex]].

[18] A. M. Sirunyan *et al.* [CMS Collaboration], "Search for an $L_\mu - L_\tau$ gauge boson using $\mathrm{Z} \to 4\mu$ events in proton-proton collisions at $\sqrt{s} = 13$ TeV," [arXiv:1808.03684 [hep-ex]].

[19] A. M. Sirunyan *et al.* [CMS Collaboration], "Search for long-lived particles with displaced vertices in multijet events in proton-proton collisions at $\sqrt{s} =$13 TeV," arXiv:1808.03078 [hep-ex].

[20] A. M. Sirunyan *et al.* [CMS Collaboration], "Search for pair-produced resonances decaying to quark pairs in proton-proton collisions at $\sqrt{s} = 13$ TeV," arXiv:1808.03124 [hep-ex].

[21] A. M. Sirunyan *et al.* [CMS Collaboration], "Evidence for the associated production of a single top quark and a photon in proton-proton collisions at $\sqrt{s} = 13$ TeV," arXiv:1808.02913 [hep-ex].

[22] A. M. Sirunyan *et al.* [CMS Collaboration], "Search for resonances in the mass spectrum of muon pairs produced in association with b quark jets in proton-proton collisions at $\sqrt{s} =$ 8 and 13 TeV," arXiv:1808.01890 [hep-ex].

[23] A. M. Sirunyan *et al.* [CMS Collaboration], "Search for production of Higgs boson pairs in the four b quark final state using large-area jets in proton-proton collisions at $\sqrt{s} = 13$ TeV," arXiv:1808.01473 [hep-ex].

[24] A. M. Sirunyan *et al.* [CMS Collaboration], "Search for heavy resonances decaying into two Higgs bosons or into a Higgs boson and a W or Z boson in proton-proton collisions at 13 TeV," arXiv:1808.01365 [hep-ex].

[25] A. M. Sirunyan *et al.* [CMS Collaboration], "Search for narrow Hγ resonances in proton-proton collisions at $\sqrt{s} = 13$ TeV," arXiv:1808.01257 [hep-ex].

[26] A. M. Sirunyan *et al.* [CMS Collaboration], "Search for a W' boson decaying to a τ lepton and a neutrino in proton-proton collisions at $\sqrt{s} = 13$ TeV," [arXiv:1807.11421 [hep-ex]].

[27] A. M. Sirunyan *et al.* [CMS Collaboration], "Searches for pair production of charginos and top squarks in final states with two oppositely charged leptons in proton-proton collisions at $\sqrt{s} = 13$ TeV," [arXiv:1807.07799 [hep-ex]].

[28] A. M. Sirunyan *et al.* [CMS Collaboration], "Search for dark matter particles produced in association with a top quark pair at $\sqrt{s} = 13$ TeV," [arXiv:1807.06522 [hep-ex]].

[29] A. M. Sirunyan *et al.* [CMS Collaboration], "Search for the Higgs boson decaying to two muons in proton-proton collisions at $\sqrt{s} = 13$ TeV," [arXiv:1807.06325 [hep-ex]].

[30] A. M. Sirunyan *et al.* [CMS Collaboration], "Measurements of the differential jet cross section as a function of the jet mass in dijet events from proton-proton collisions at $\sqrt{s} = 13$ TeV," arXiv:1807.05974 [hep-ex].

[31] A. M. Sirunyan *et al.* [CMS Collaboration], "Measurement of inclusive and differential Higgs boson production cross sections in the diphoton decay channel in proton-proton collisions at $\sqrt{s} = 13$ TeV," arXiv:1807.03825 [hep-ex].

[32] A. M. Sirunyan *et al.* [CMS Collaboration], "Precision measurement of the structure of the CMS inner tracking system using nuclear interactions," [arXiv:1807.03289 [physics.ins-det]].

[33] A. M. Sirunyan *et al.* [CMS Collaboration], "Search for heavy resonances decaying into a vector boson and a Higgs boson in final states with charged leptons, neutrinos and b quarks at $\sqrt{s} = 13$ TeV," arXiv:1807.02826 [hep-ex].

[34] A. M. Sirunyan *et al.* [CMS Collaboration], "Study of the underlying event in top quark pair production in pp collisions at 13 TeV," arXiv:1807.02810 [hep-ex].

[35] A. M. Sirunyan *et al.* [CMS Collaboration], "Search for supersymmetry in events with a τ lepton pair and missing transverse momentum in proton-proton collisions at $\sqrt{s} = 13$ TeV," arXiv:1807.02048 [hep-ex].

[36] A. M. Sirunyan *et al.* [CMS Collaboration], "Measurement of differential cross sections for inclusive isolated-photon and photon+jets production in proton-proton collisions at $\sqrt{s} = 13$ TeV," arXiv:1807.00782 [hep-ex].

[37] A. M. Sirunyan *et al.* [CMS Collaboration], "Measurement of charged particle spectra in minimum-bias events from protonproton collisions at $\sqrt{s} = 13\,\text{TeV}$," Eur. Phys. J. C **78**, no. 9, 697 (2018) doi:10.1140/epjc/s10052-018-6144-y [arXiv:1806.11245 [hep-ex]].

[38] A. M. Sirunyan *et al.* [CMS Collaboration], "Measurement of differential cross sections for Z boson pair production in association with jets at $\sqrt{s} = 8$ and 13 TeV," arXiv:1806.11073 [hep-ex].

[39] A. M. Sirunyan *et al.* [CMS Collaboration], "Search for heavy Majorana neutrinos in same-sign dilepton channels in proton-proton collisions at $\sqrt{s} = 13$ TeV," arXiv:1806.10905 [hep-ex].

[40] A. M. Sirunyan *et al.* [CMS Collaboration], "Search for the decay of a Higgs boson in the $\ell\ell\gamma$ channel in proton-proton collisions at $\sqrt{s} = 13$ TeV," [arXiv:1806.05996 [hep-ex]].

[41] A. M. Sirunyan *et al.* [CMS Collaboration], "Search for supersymmetric partners of electrons and muons in proton-proton collisions at $\sqrt{s} = 13$ TeV," [arXiv:1806.05264 [hep-ex]].

[42] A. M. Sirunyan *et al.* [CMS Collaboration], "Measurements of properties of the Higgs boson decaying to a W boson pair in pp collisions at $\sqrt{s} = 13$ TeV," [arXiv:1806.05246 [hep-ex]].

[43] A. M. Sirunyan *et al.* [CMS Collaboration], "Search for dark matter produced in association with a Higgs boson decaying to $\gamma\gamma$ or $\tau^+\tau^-$ at $\sqrt{s} = 13$ TeV," JHEP **1809**, 046 (2018) doi:10.1007/JHEP09(2018)046 [arXiv:1806.04771 [hep-ex]].

[44] A. M. Sirunyan *et al.* [CMS Collaboration], "Observation of the Z$\to \psi\ell^+\ell^-$ decay in pp collisions at $\sqrt{s} = 13$ TeV," Phys. Rev. Lett. **121**, 141801 (2018) doi:10.1103/PhysRevLett.121.141801 [arXiv:1806.04213 [hep-ex]].

[45] A. M. Sirunyan *et al.* [CMS Collaboration], "Search for resonant pair production of Higgs bosons decaying to bottom quark-antiquark pairs in proton-proton collisions at 13 TeV," JHEP **1808**, 152 (2018) doi:10.1007/JHEP08(2018)152 [arXiv:1806.03548 [hep-ex]].

[46] A. M. Sirunyan *et al.* [CMS Collaboration], "Search for a singly produced third-generation scalar leptoquark decaying to a τ lepton and a bottom quark in proton-proton collisions at $\sqrt{s} = 13$ TeV," JHEP **1807**, 115 (2018) doi:10.1007/JHEP07(2018)115 [arXiv:1806.03472 [hep-ex]].

[47] A. M. Sirunyan *et al.* [CMS Collaboration], "Search for pair-produced resonances each decaying into at least four quarks in proton-proton collisions at $\sqrt{s} = 13$ TeV," Phys. Rev. Lett. **121**, 141802 (2018) doi:10.1103/PhysRevLett.121.141802 [arXiv:1806.01058 [hep-ex]].

[48] A. M. Sirunyan *et al.* [CMS Collaboration], "Measurement of the weak mixing angle using the forward-backward asymmetry of Drell-Yan events in pp collisions at 8 TeV," Eur. Phys. J. C **78**, 701 (2018) doi:10.1140/epjc/s10052-018-6148-7 [arXiv:1806.00863 [hep-ex]].

[49] A. M. Sirunyan *et al.* [CMS Collaboration], "Search for narrow and broad dijet resonances in proton-proton collisions at $\sqrt{s} = 13$ TeV and constraints on dark matter mediators and other new particles," JHEP **1808**, 130 (2018) doi:10.1007/JHEP08(2018)130 [arXiv:1806.00843 [hep-ex]].

[50] A. M. Sirunyan *et al.* [CMS Collaboration], "Search for beyond the standard model Higgs bosons decaying into a $\mathrm{b\bar{b}}$ pair in pp collisions at $\sqrt{s} = 13$ TeV," JHEP **1808**, 113 (2018) doi:10.1007/JHEP08(2018)113 [arXiv:1805.12191 [hep-ex]].

[51] A. M. Sirunyan *et al.* [CMS Collaboration], "Observation of the $\chi_{\mathrm{b1}}(3\mathrm{P})$ and $\chi_{\mathrm{b2}}(3\mathrm{P})$ and measurement of their masses," Phys. Rev. Lett. **121**, 092002 (2018) doi:10.1103/PhysRevLett.121.092002 [arXiv:1805.11192 [hep-ex]].

[52] A. M. Sirunyan *et al.* [CMS Collaboration], "Constraints on models of scalar and vector leptoquarks decaying to a quark and a neutrino at $\sqrt{s} = 13$ TeV," Phys. Rev. D **98**, no. 3, 032005 (2018) doi:10.1103/PhysRevD.98.032005 [arXiv:1805.10228 [hep-ex]].

[53] A. M. Sirunyan *et al.* [CMS Collaboration], "Search for an exotic decay of the Higgs boson to a pair of light pseudoscalars in the final state with two b quarks and two τ leptons in proton-proton collisions at $\sqrt{s} = 13$ TeV," Phys. Lett. B **785**, 462 (2018) doi:10.1016/j.physletb.2018.08.057 [arXiv:1805.10191 [hep-ex]].

[54] A. M. Sirunyan *et al.* [CMS Collaboration], "Measurement of the production cross section for single top quarks in association with W bosons in proton-proton collisions at $\sqrt{s} = 13$ TeV," [arXiv:1805.07399 [hep-ex]].

[55] A. M. Sirunyan *et al.* [CMS Collaboration], "Search for black holes and sphalerons in high-multiplicity final states in proton-proton collisions at $\sqrt{s} = 13$ TeV," arXiv:1805.06013 [hep-ex].

[56] A. M. Sirunyan *et al.* [CMS Collaboration], "Search for top squarks decaying via four-body or chargino-mediated modes in single-lepton final states in proton-proton collisions at $\sqrt{s} = 13$ TeV," JHEP **1809**, 065 (2018) doi:10.1007/JHEP09(2018)065 [arXiv:1805.05784 [hep-ex]].

[57] A. M. Sirunyan *et al.* [CMS Collaboration], "Measurement of the groomed jet mass in PbPb and pp collisions at $\sqrt{s_{\mathrm{NN}}} = 5.02$ TeV," arXiv:1805.05145 [hep-ex].

[58] A. M. Sirunyan *et al.* [CMS Collaboration], "Search for an exotic decay of the Higgs boson to a pair of light pseudoscalars in the final state of two muons and two τ leptons in proton-proton collisions at $\sqrt{s} = 13$ TeV," arXiv:1805.04865 [hep-ex].

[59] A. M. Sirunyan *et al.* [CMS Collaboration], "Search for vector-like T and B quark pairs in final states with leptons at $\sqrt{s} = 13$ TeV," JHEP **1808**, 177 (2018) doi:10.1007/JHEP08(2018)177 [arXiv:1805.04758 [hep-ex]].

[60] A. M. Sirunyan *et al.* [CMS Collaboration], "Constraining gluon distributions in nuclei using dijets in proton-proton and proton-lead collisions at $\sqrt{s_{\mathrm{NN}}} = 5.02$ TeV," Phys. Rev. Lett. **121**, no. 6, 062002 (2018) doi:10.1103/PhysRevLett.121.062002 [arXiv:1805.04736 [hep-ex]].

[61] A. M. Sirunyan *et al.* [CMS Collaboration], "Measurement of prompt $\psi(2S)$ production cross sections in proton-lead and proton-proton collisions at $\sqrt{s_{\mathrm{NN}}} = 5.02$ TeV," arXiv:1805.02248 [hep-ex].

[62] A. M. Sirunyan *et al.* [CMS Collaboration], "Measurement of the top quark mass with lepton+jets final states using pp collisions at $\sqrt{s} = 13$ TeV," arXiv:1805.01428 [hep-ex].

[63] A. M. Sirunyan *et al.* [CMS Collaboration], "Elliptic flow of charm and strange hadrons in high-multiplicity pPb collisions at $\sqrt{s_{\mathrm{NN}}} = 8.16$ TeV," Phys. Rev. Lett. **121**, no. 8, 082301 (2018) doi:10.1103/PhysRevLett.121.082301 [arXiv:1804.09767 [hep-ex]].

[64] A. M. Sirunyan *et al.* [CMS Collaboration], "Search for disappearing tracks as a signature of new long-lived particles in proton-proton collisions at $\sqrt{s} = 13$ TeV," JHEP **1808**, 016 (2018) doi:10.1007/JHEP08(2018)016 [arXiv:1804.07321 [hep-ex]].

[65] A. M. Sirunyan *et al.* [CMS Collaboration], "Measurement of differential cross sections for Z boson production in association with jets in proton-proton collisions at $\sqrt{s} = 13$ TeV," arXiv:1804.05252 [hep-ex].

[66] A. M. Sirunyan *et al.* [CMS Collaboration], "Search for $\mathrm{t\bar{t}H}$ production in the $H \to \mathrm{b\bar{b}}$ decay channel with leptonic $\mathrm{t\bar{t}}$ decays in proton-proton collisions at $\sqrt{s} = 13$ TeV," arXiv:1804.03682 [hep-ex].

[67] A. M. Sirunyan *et al.* [CMS Collaboration], "Measurements of Higgs boson properties in the diphoton decay channel in proton-proton collisions at $\sqrt{s} = 13$ TeV," arXiv:1804.02716 [hep-ex].

[68] A. M. Sirunyan *et al.* [CMS Collaboration], "Observation of $\mathrm{t\bar{t}H}$ production," Phys. Rev. Lett. **120**, no. 23, 231801 (2018) doi:10.1103/PhysRevLett.120.231801, 10.1130/PhysRevLett.120.231801 [arXiv:1804.02610 [hep-ex]].

[69] A. M. Sirunyan *et al.* [CMS Collaboration], "Search for a new scalar resonance decaying to a pair of Z bosons in proton-proton collisions at $\sqrt{s} = 13$ TeV," JHEP **1806**, 127 (2018) doi:10.1007/JHEP06(2018)127 [arXiv:1804.01939 [hep-ex]].

[70] A. M. Sirunyan *et al.* [CMS Collaboration], "Search for high-mass resonances in final states with a lepton and missing transverse momentum at $\sqrt{s} = 13$ TeV," JHEP **1806**, 128 (2018) doi:10.1007/JHEP06(2018)128 [arXiv:1803.11133 [hep-ex]].

[71] A. M. Sirunyan *et al.* [CMS Collaboration], "Search for a heavy right-handed W boson and a heavy neutrino in events with two same-flavor leptons and two jets at $\sqrt{s} = 13$ TeV," JHEP **1805**, no. 05, 148 (2018) doi:10.1007/JHEP05(2018)148 [arXiv:1803.11116 [hep-ex]].

[72] A. M. Sirunyan *et al.* [CMS Collaboration], "Search for a heavy resonance decaying into a Z boson and a Z or W boson in 22q final states at $\sqrt{s} = 13$ TeV," JHEP **1809**, 101 (2018) doi:10.1007/JHEP09(2018)101 [arXiv:1803.10093 [hep-ex]].

[73] A. M. Sirunyan *et al.* [CMS Collaboration], "Measurement of differential cross sections for the production of top quark pairs and of additional jets in lepton+jets events from pp collisions at $\sqrt{s} = 13$ TeV," Phys. Rev. D **97**, no. 11, 112003 (2018) doi:10.1103/PhysRevD.97.112003 [arXiv:1803.08856 [hep-ex]].

[74] A. M. Sirunyan *et al.* [CMS Collaboration], "Search for new physics in dijet angular distributions using protonproton collisions at $\sqrt{s} = 13$ TeV and constraints on dark matter and other models," Eur. Phys. J. C **78**, no. 9, 789 (2018) doi:10.1140/epjc/s10052-018-6242-x [arXiv:1803.08030 [hep-ex]].

[75] A. M. Sirunyan *et al.* [CMS Collaboration], "Search for $\mathrm{t\bar{t}H}$ production in the all-jet final state in proton-proton collisions at $\sqrt{s} = 13$ TeV," JHEP **1806**, 101 (2018) doi:10.1007/JHEP06(2018)101 [arXiv:1803.06986 [hep-ex]].

[76] A. M. Sirunyan *et al.* [CMS Collaboration], "Search for additional neutral MSSM Higgs bosons in the $\tau\tau$ final state in proton-proton collisions at $\sqrt{s} = 13$ TeV," JHEP **1809**, 007 (2018) doi:10.1007/JHEP09(2018)007 [arXiv:1803.06553 [hep-ex]].

[77] A. M. Sirunyan *et al.* [CMS Collaboration], "Search for high-mass resonances in dilepton final states in proton-proton collisions at $\sqrt{s} = 13$ TeV," JHEP **1806**, 120 (2018) doi:10.1007/JHEP06(2018)120 [arXiv:1803.06292 [hep-ex]].

[78] A. M. Sirunyan *et al.* [CMS Collaboration], "Evidence for associated production of a Higgs boson with a top quark pair in final states with electrons, muons, and hadronically decaying τ leptons at $\sqrt{s} = 13$ TeV," JHEP **1808**, 066 (2018) doi:10.1007/JHEP08(2018)066 [arXiv:1803.05485 [hep-ex]].

[79] A. M. Sirunyan *et al.* [CMS and TOTEM Collaborations], "Observation of proton-tagged, central (semi)exclusive production of high-mass lepton pairs in pp collisions at 13 TeV with the CMS-TOTEM precision proton spectrometer," JHEP **1807**, 153 (2018) doi:10.1007/JHEP07(2018)153 [arXiv:1803.04496 [hep-ex]].

[80] A. M. Sirunyan *et al.* [CMS Collaboration], "Jet properties in PbPb and pp collisions at $\sqrt{s_{\mathrm{N\,N}}} = 5.02$ TeV," JHEP **1805**, 006 (2018) doi:10.1007/JHEP05(2018)006 [arXiv:1803.00042 [nucl-ex]].

[81] A. M. Sirunyan *et al.* [CMS Collaboration], "Search for a heavy resonance decaying to a pair of vector bosons in the lepton plus merged jet final state at $\sqrt{s} = 13$ TeV," JHEP **1805**, 088 (2018) doi:10.1007/JHEP05(2018)088 [arXiv:1802.09407 [hep-ex]].

[82] A. M. Sirunyan *et al.* [CMS Collaboration], "Search for narrow resonances in the b-tagged dijet mass spectrum in proton-proton collisions at $\sqrt{s} = 8$ TeV," Phys. Rev. Lett. **120**, no. 20, 201801 (2018) doi:10.1103/PhysRevLett.120.201801 [arXiv:1802.06149 [hep-ex]].

[83] A. M. Sirunyan *et al.* [CMS Collaboration], "Search for natural and split supersymmetry in proton-proton collisions at $\sqrt{s} = 13$ TeV in final states with jets and missing transverse momentum," JHEP **1805**, 025 (2018) doi:10.1007/JHEP05(2018)025 [arXiv:1802.02110 [hep-ex]].

[84] A. M. Sirunyan *et al.* [CMS Collaboration], "Search for lepton-flavor violating decays of heavy resonances and quantum black holes to e final states in proton-proton collisions at $\sqrt{s} = 13$ TeV," JHEP **1804**, 073 (2018) doi:10.1007/JHEP04(2018)073 [arXiv:1802.01122 [hep-ex]].

[85] A. M. Sirunyan *et al.* [CMS Collaboration], "Comparing transverse momentum balance of b jet pairs in pp and PbPb collisions at $\sqrt{s_{\mathrm{NN}}} = 5.02$ TeV," JHEP **1803**, 181 (2018) doi:10.1007/JHEP03(2018)181 [arXiv:1802.00707 [hep-ex]].